forests

MDPI

Article

Evaluation of Wood Anatomical Properties from 18 Tree Species in the Subtropical Region of China

Yunpeng Wang [1], Yiping Wang [2], Le Shen [1], Zhaoxiang Wu [1], Huihu Li [1], Miao Hu [1], Qiaoli Liu [1], Caihui Chen [1], Xiaokang Hu [3,*] and Yongda Zhong [1,*]

[1] Engineering Research Center of Genetic Improvement and Cultivation of Native Precious Broad-Leaved Tree Species of Jiangxi Province, Institute of Biological Resources, Jiangxi Academy of Sciences, Nanchang 330096, China; wypcnsd@163.com (Y.W.); shenle2023@126.com (L.S.); wuzhaoxiang2004@126.com (Z.W.); lhh26521@163.com (H.L.); humiao29@163.com (M.H.); liuqiaoli2019@126.com (Q.L.); chencaihui0110@163.com (C.C.)
[2] Gannan Arboretum, Ganzhou 341299, China; wangyp_1223@163.com
[3] Ganzhou Institute of Forestry, Ganzhou 341212, China
* Correspondence: kang123878@163.com (X.H.); zhongyongda@jxas.ac.cn (Y.Z.)

Abstract: The subtropical region of China possesses abundant broad-leaf tree species resources; however, the anatomical properties and microstructure of the wood are still unclear, which restricts the processing and utilization of wood. In this study, 14 broad-leaf trees and four coniferous trees were selected. Wood anatomical indices and wood microanatomy were used to evaluate the wood properties using a comprehensive index method. The results have shown that *Dalbergia assamica* exhibited the highest wood basic density among the 14 broad-leaved tree species, accompanied by a significant fiber proportion and vessel lumen diameter but a small vessel proportion and a high number of wood rays. Conversely, *Parakmeria lotungensis* and *Michelia chapensis* had relatively low wood basic densities, rendering them less suitable as valuable broad-leaved wood sources. *Altingia chinensis*, *Castanopsis kawakamii*, and the remaining 11 tree species exhibited medium-level wood basic densities. The 14 broad-leaved tree species had medium-length fibers. *Phoebe bournei*, *Dalbergia assamica*, and *Castanopsis kawakamii* demonstrated relatively high fiber proportion. *Altingia chinensis*, *Dalbergia assamica*, and *Castanopsis kawakamii* exhibited a large number of wood rays, making their wood more susceptible to cracking, whereas other broad-leaved tree species possessed fewer wood rays. The findings have provided a scientific basis for the exploration of precious broad-leaved tree resources and wood use.

Keywords: broad-leaved trees; wood basic density; wood anatomical characteristics; fibers; vessels

Citation: Wang, Y.; Wang, Y.; Shen, L.; Wu, Z.; Li, H.; Hu, M.; Liu, Q.; Chen, C.; Hu, X.; Zhong, Y. Evaluation of Wood Anatomical Properties from 18 Tree Species in the Subtropical Region of China. *Forests* **2023**, *14*, 2344. https://doi.org/10.3390/f14122344

Academic Editor: Ian Hartley

Received: 10 October 2023
Revised: 6 November 2023
Accepted: 27 November 2023
Published: 29 November 2023

1. Introduction

Wood is an essential and renewable natural material crucial for economic development and human life. However, with improvements in living standards, the market supply of bulk wood is insufficient to meet human needs [1]. Known for their exceptional qualities, such as high hardness, deep color, and beautiful texture, precious woods are highly favored by people and are primarily used for high-end furniture, decoration, and wooden crafts [2]. This is particularly true for the increasing demand for large-diameter precious broad-leaf wood [3,4]. Although China's total forest resources have been increasing, timber resources for logging remain scarce [5]. Since 1998, China has implemented natural forest protection projects that have substantially reduced the production of precious wood and large-diameter timber. To meet this demand, China relies heavily on the importation of high-end precious wood from Southeast Asia and South Africa [1,6]. However, these countries have strengthened their ecological protection, resulting in restrictions on international timber exports [4,6]. Consequently, relying on imported precious wood is not a sustainable long-term solution considering China's national strength and the international timber

market. To address the supply and demand conflict in the Chinese timber industry, it is imperative to rely on domestic reserve resources, actively develop precious wood, cultivate large-diameter timber, and increase the national strategic timber reserves.

The anatomical properties of wood determine the processing and use of timber. In terms of the anatomical properties of timber, fibers and vessels are the main structural units of broad-leaf materials. Their size, quantity, and structure are closely related to the physical properties of the timber and directly determine the value of timber use [7,8]. The microfibril angle refers to the angle formed by the arrangement of microfibrils in the secondary cell wall S2 layer of plant cells and the cell axis. The microfibril angle is closely related to the physical and mechanical properties of wood fibers. The microfibril angle affects the strength of the fibers [9,10], directly influencing the elastic modulus and anisotropic shrinkage of wood [11]. Therefore, understanding the microstructure of wood is of considerable importance for its processing and use. However, to date, studies on the properties of precious tree species have mainly focused on the basic wood density. Meanwhile, there has been relatively little research on the anatomical microstructure of wood. Therefore, the anatomical properties of wood remain unclear. This study used wood from 14 broad-leaf trees and four coniferous trees to measure wood anatomical parameters and observe the wood microstructure. The wood properties of 18 tree species were evaluated in detail, providing quality parameters for the processing and use of valuable timber and theoretical guidance for directional cultivation.

2. Materials and Methods

2.1. Plant Materials

The tree species used in the experiment were sourced from the Gannan Arboretum in Jiangxi Province (114°22′, 25°51′). The region has a subtropical humid monsoon climate, with an average annual temperature of 18.8 °C, an average annual sunshine duration of 1765.2 h, a frost-free period of 289 d, and an average annual rainfall of 1497 mm. There were 18 tree species included in the experiment, including 14 broad-leaf and four coniferous species (Table 1). For each tree species, 5–35 well-grown trees were selected, and two defect-free wood cores from the pith to the bark were obtained at an uphill position with a diameter of 5 mm using a growth cone drill. The wood samples were taken back to the laboratory to determine their properties. One of the wooden cores was placed in FAA fixative for preservation and used to observe the wood microstructure. The other wood core was stored at room temperature, brought back to the laboratory, and used for the determination of the wood samples' anatomical properties.

Table 1. Tree species information.

No.	Tree Species	Family	Age	The Number of Individual Plants	Diameter at Breast Height (cm)
1	*Dalbergia assamica* Benth.	Fabaceae	50	5	32.80 ± 3.50
2	*Altingia chinensis* (Champ.) Oliver ex Hance	Hamamelidaceae	39	10	21.67 ± 3.36
3	*Castanopsis kawakamii* Hayata	Fagaceae	35	5	20.34 ± 3.43
4	*Michelia macclurei* Dandy	Magnoliaceae	40	5	25.42 ± 3.02
5	*Michelia fallaxa* Dandy	Magnoliaceae	37	5	20.40 ± 1.85
6	*Cinnamomum camphora* (L.) Presl	Lauraceae	35	5	28.13 ± 2.35
7	*Manglietia fordiana* Oliv.	Magnoliaceae	38	5	23.00 ± 9.63
8	*Nyssa sinensis* Oliv.	Nyssaceae	42	5	17.82 ± 4.95
9	*Mytilaria laosensis* Lec.	Hamamelidaceae	36	5	27.58 ± 3.58
10	*Michelia foveolata* Merr. Ex Dandy	Magnoliaceae	37	5	14.72 ± 2.64
11	*Phoebe bournei* (Hemsl.) Yang	Lauraceae	31	5	23.78 ± 5.18
12	*Parakmeria lotungensis* (Chun et C. Tsoong) Law	Magnoliaceae	36	5	20.48 ± 2.69
13	*Michelia chapensis* Dandy	Magnoliaceae	37	5	17.94 ± 2.12
14	*Michelia odora* (Chun) Nooteboom and B. L. Chen	Magnoliaceae	38	35	23.71 ± 10.08
15	*Chamaecyparis pisifera* cv. plumosa	Cupressaceae	34	5	26.00 ± 3.15
16	*Fokienia hodginsii* (Dunn) A. Henry et Thomas	Cupressaceae	40	10	25.52 ± 4.59
17	*Taiwania cryptomerioides* Hayata	Cupressaceae	36	5	25.38 ± 4.03
18	*Cupressus lusitanica* 'zhongshanbai'	Cupressaceae	39	5	19.50 ± 1.94

2.2. Measurements of Wood Anatomical Properties

The basic wood density (WBD) was determined using the maximum moisture content method [12]. Assessment of fiber and vessel morphology was performed by disassociating them in a dissociation solution with 30% hydrogen peroxide to glacial acetic acid ratio of 1:1 in a boiling water bath at 90 °C for 4 h. The disassociated tissues were rinsed in distilled water until all the dissociation solutions were completely washed away. Subsequently, the rinsed tissues were crushed in water and stained with safranin (1%) to create temporary slices, which were observed and photographed under a microscope. Each sample was analyzed using ImageJ (v1.52) software to randomly measure 50 intact wood fibers and vessels. The measured parameters included fiber length, fiber width, vessel length, and vessel width.

After allowing the wood core to preserve for 72 h in FAA fixative, samples were taken from 3 to 8 growth rings near the bark. The samples were then softened and sliced to a thickness of 15–20 um using a semi-automatic sliding microtome. A double staining method involving safranin red and fast green was used. The samples were stained with 1% safranin red for 15 min, followed by staining with 0.5% fast green for 15 s. This process was then repeated. To complete the process, the slices were subjected to alcohol gradient dehydration ranging from 50% to 100% and sealed with a neutral resin. The sections were observed under an optical microscope (Zeiss, Imager A2, Oberkochen, Germany), and the fiber tissue proportion, vessel tissue proportion, vessel lumen area, and double cell wall thickness were measured using ImageJ software (v1.52). The width of the wood rays was measured. The number of wood rays within 5 mm was calculated.

Thin slices of the outermost latewood (located close to the bark) of each wood core were taken, with a thickness of approximately 1 mm. Measurements were conducted using the X-ray diffraction method, employing the Japanese RIGAKU Ultima IV X-ray diffraction instrument. The instrument was set to a voltage of 40 kV and a current of 40 mA. The X-ray beam had a cross-section of 4 m × 2 m, with a 2θ angle of 22.6°. The sample was rotated at an angle of 180° during the scanning process, resulting in a diffraction intensity curve for the obtained experimental sample. The microfibril angle was calculated using the 0.6T method [9].

2.3. Data Analyses

Wood basic density was calculated according to the following formula:

$$\mathrm{P} = 1/[(M - M_0)/M_0 + 1/D_w \quad (1)$$

where M is the weight (g) of the sample at the saturated moisture content, M_0 is the weight (g) for the oven-dried sample, and D_w is the specific gravity of the wood material that forms the cell wall with an average value of 1.53.

The correlation coefficient was calculated according to the following formula:

$$r = Cov(x,\ y)/\sqrt{\sigma_x^2 \cdot \sigma_y^2} \quad (2)$$

where $Cov(x, y)$ is the covariance of the wood properties x and y, and σ_x^2 and σ_y^2 are the variance of the wood properties x and y, respectively. The method for selecting the comprehensive index for multiple traits is referred to as the Smith–Hazel method [13].

$$I = \sum_{i=1}^{n} w_n P_n \quad (3)$$

$$w_n = 1/\sigma \quad (4)$$

where I is the value of the comprehensive selection index, w_n is the economic weight of the nth trait, P_n is the phenotype value of the nth trait, and σ is the standard deviation of the nth trait.

3. Results

3.1. Wood Anatomical Properties of Different Tree Species

There were differences in the basic density and anatomical characteristics of wood among the different tree species (Table 2). The wood basic density of *Dalbergia assamica* was the highest among the 14 broad-leaved trees, with 0.8786 g·cm^{-3}. The wood basic density of *Michelia odora* and *Michelia chapensis* was similar to that of coniferous trees (Table 2), with values of 0.4372 g·cm^{-3} and 0.4392 g·cm^{-3}, respectively. The wood basic density of the remaining 11 broad-leaved trees was at a medium level, ranging from 0.5138 g·cm^{-3} to 0.6812 g·cm^{-3}. The wood basic density of the four coniferous trees was below 0.5 g·cm^{-3}, ranging from 0.3554 g·cm^{-3} to 0.4698 g·cm^{-3} (Table 2), all of which were lower than that of the 14 broad-leaved trees.

Trees with high basic density do not necessarily have thick cell walls. *Altingia chinensis*, ranked second in terms of basic wood density, had the thickest double cell wall, measuring 15.88 µm. *Mytilaria laosensis* was ranked ninth and had the second thickest double cell wall (11.37 µm). The tree with the highest basic density, namely, *Dalbergia assamica*, had a relatively small double cell wall thickness of 5.93 µm. *Cinnamomum camphora* had the smallest double cell wall thickness, with 5.47 µm. Among the coniferous trees (Table 2), *Cupressus lusitanica* had the lowest basic density (0.3554 g·cm^{-3}), but it also had a larger double cell wall thickness (13.61 µm).

The fibers of the tested 14 broad-leaved trees had a medium length (Table 2), ranging from 971.91 µm to 1616.24 µm and tracheids of the four coniferous trees ranged from 1519.01 µm to 1944.15 µm (Table 2). The fiber width of the broad-leaved trees ranged from 20.95 µm to 30.76 µm. This was smaller than the tracheid width of the coniferous trees, which ranged from 24.81 µm to 44.58 µm. The fiber length-to-width ratio was between 40.88 and 62.53, which was similar to the tracheid length-to-width ratio of the coniferous trees, which ranged from 45.00 to 64.35. *Altingia chinensis* had the longest fibers at 1616.24 µm and the largest fiber length-to-width ratio of 62.53. However, a relatively small fiber tissue proportion (57.34%) indicated that its fibers were long and thick, but they were fewer in quantity. *Mytilaria laosensis* had the second longest fiber length (1581.30 µm) and a moderate length-to-width ratio (54.44), indicating that it had relatively fine fibers. *Castanopsis kawakamii* had the shortest fiber length (866.17 µm) and the smallest length-to-width ratio (40.88). However, it had a larger fiber tissue proportion (72.65%), indicating that the fibers were short and thin but also greater in quantity. *Phoebe bournei* and *Dalbergia assamica* had relatively large fiber tissue proportions, with 74.16% and 72.70%, respectively. However, their fiber lengths were relatively small, measuring 1014.95 µm and 971.91 µm, respectively. The fiber proportions of the other broad-leaved tree species varied from 55.47% to 65.97%, indicating medium levels.

The results of vessel measurements (Table 2) showed significant differences in vessel length among the 14 broad-leaved trees, ranging from 235.83 µm to 1330.12 µm, with the longest vessel being approximately 5.64 times longer than the shortest vessel. The vessel widths ranged from 67.38 µm to 141.66 µm, with the largest vessel width being approximately 2.10 times wider than the smallest vessel width. Among them, *Dalbergia assamica* had the largest lumen area of vessels (16,139.80 µm^2), but it had the shortest vessel length (235.85 µm), the smallest length-to-width ratio (3.55), and the smallest vessel tissue proportion (4.36%). This indicated that the vessels of *Dalbergia assamica* were thick, short, and have a large lumen area, but they were fewer in quantity. *Cinnamomum camphora* had the second largest lumen area of vessels (9399.97 µm^2), but shorter vessels (500.56 µm), and the largest vessel width (141.66 µm), with a moderate vessel tissue proportion (11.96%) and a relatively small length-to-width ratio (3.84). This indicated that the vessels of *Cinnamomum camphora* were short, thick, and less in quantity. *Mytilaria laosensis* had the longest vessels (1330.12 µm), the highest length-to-width ratio (18.27), relatively large vessel tissue proportion (25.67%), and a moderate lumen area of vessels (2362.18 µm^2). This indicated that *Mytilaria laosensis* had relatively slender and long vessels with a higher quantity. The vessel lengths of the other broad-leaved tree species ranged from 488.55 µm to 955.32 µm,

all of which were found to be of medium length, and the vessel proportions ranged from 9.40 to 23.70, while the lumen areas of vessels ranged from 1257.35 μm^2 to 2679.74 μm^2.

The results showed that the microfibril angle did not differ significantly among the 14 broad-leaved trees (Table 2), ranging from 11.42° to 14.96°, with an average value of 13.25°, which was smaller than the average value of the microfibril angle in the four coniferous trees (21.20°). Among the broad-leaved tree species, *Michelia foveolata* (14.96°), *Manglietia fordiana* (14.57°), *Cinnamomum camphora* (14.20°), *Parakmeria lotungensis* (14.15°), and *Phoebe bournei* (14.04°) had microfibril angles above 14°. *Nyssa sinensis* (11.42°), *Mytilaria laosensis* (11.63°), and *Castanopsis kawakamii* (11.68°) had the smallest microfibril angles. Among the coniferous trees (Table 2), *Cupressus lusitanica* had the smallest basic wood density, with short and narrow tracheids, but it had the largest vessel lumen area, double cell wall thickness, and largest microfibril angle (32.74°). *Taiwania cryptomerioides* had long and thick tracheids with the smallest microfibril angle (12.09°).

3.2. Wood Microstructure

The microscopic section results (Figure 1, Table 3) showed that the vessel pore compound mode of the tested broad-leaf tree species was composed of three main types; that is, solitary pores, multiple pores, and pore clusters. Most tree species exhibit a combination of these types, whereas only a few species exhibit a single type. *Altingia chinensis* and *Phoebe bournei* have vessel pores primarily of the solitary pore type. *Dalbergia assamica*, *Castanopsis kawakamii*, and *Mytilaria laosensis* mainly possessed solitary pores, although a small number of multiple pores were also present. *Michelia macclurei* and *Michelia fallaxa* predominantly had multiple pores. *Cinnamomum camphora* was characterized by typical pore clusters, with large pores in the center and small pores on the periphery. *Parakmeria lotungensis*, *Michelia chapensis*, and *Parakmeria lotungensis*, which have relatively low wood densities, had a combination of multiple pores and pore clusters. The arrangement of the vessel pores in the tested broad-leaf tree species was predominantly dispersed. *Castanopsis kawakamii* exhibited an apsacline arrangement of vessels, whereas *Mytilaria laosensis* exhibited a radial arrangement.

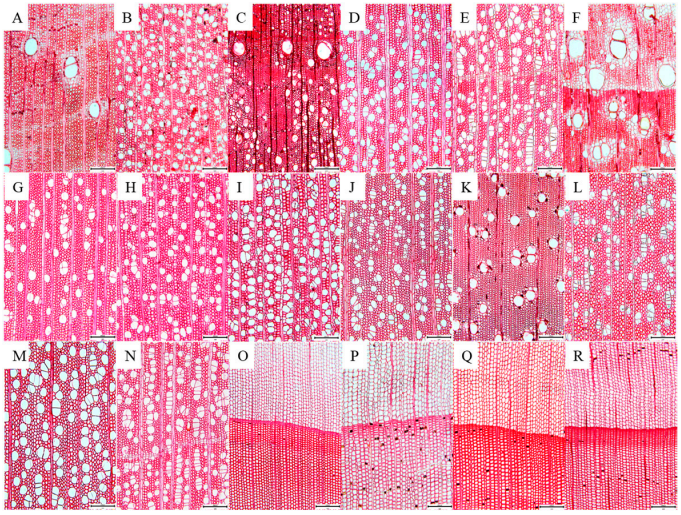

Figure 1. Wood anatomical microstructure of 18 tree species. Note: The photos of tree species were arranged in a manner that follows a decreasing order of wood basic density. (**A**) *Dalbergia assamica*, (**B**) *Altingia chinensis*, (**C**) *Castanopsis kawakamii*, (**D**) *Michelia macclurei*, (**E**) *Michelia fallaxa*, (**F**) *Cinnamomum camphora*, (**G**) *Manglietia fordiana*, (**H**) *Nyssa sinensis*, (**I**) *Mytilaria laosensis*, (**J**) *Michelia foveolata*, (**K**) *Phoebe bournei*, (**L**) *Parakmeria lotungensis*, (**M**) *Michelia chapensis*, (**N**) *Michelia odora*, (**O**) *Chamaecyparis pisifera*, (**P**) *Fokienia hodginsii*, (**Q**) *Taiwania cryptomerioides*, and (**R**) *Cupressus lusitanica*.

Table 2. Analysis of wood anatomical traits of 14 broad-leaf trees.

	Trees	Wood Basic Density ($g \cdot cm^{-3}$)	Cell Wall (μm)	Fiber/Tracheid Length (μm)	Fiber/Tracheid Width (μm)	Fiber/Tracheid Length-Width Ratio	Fiber Proportion (%)	Vessel Length (μm)	Vessel Width (μm)	Vessel Length-Width Ratio	Vessel Proportion (%)	Vessel/Tracheid Lumen Area (μm^2)	Microfibril Angle (°)
Broad-leaf trees	*Dalbergia assamica*	0.8786 ± 0.12	5.93 ± 0.69	971.91 ± 198.4	22.43 ± 1.77	45.27 ± 9.57	72.70 ± 3.04	235.83 ± 10.73	109.11 ± 64.70	3.55 ± 2.88	4.36 ± 2.06	16139.80 ± 7392.22	12.18 ± 1.21
	Altingia chinensis	0.6812 ± 0.07	15.88 ± 1.54	1616.24 ± 313.13	26.80 ± 2.18	62.53 ± 13.12	57.34 ± 4.36	955.32 ± 316.33	67.38 ± 6.15	14.85 ± 5.44	20.97 ± 4.33	1917.27 ± 494.67	12.53 ± 5.16
	Castanopsis kawakamii	0.6520 ± 0.04	6.70 ± 1.01	866.17 ± 74.72	22.37 ± 2.83	40.88 ± 6.33	72.65 ± 1.35	672.68 ± 175.93	80.24 ± 23.69	9.83 ± 3.84	11.05 ± 1.85	1821.71 ± 429.38	11.68 ± 2.54
	Michelia macclurei	0.6190 ± 0.07	7.57 ± 1.03	1384.05 ± 75.58	25.57 ± 1.76	56.28 ± 4.19	57.67 ± 5.30	786.87 ± 43.77	77.23 ± 7.69	10.74 ± 1.19	21.44 ± 3.82	2310.69 ± 424.95	13.74 ± 1.39
	Michelia fallaxa	0.6074 ± 0.08	8.97 ± 2.02	1338.66 ± 231.37	25.79 ± 2.97	53.47 ± 8.85	56.07 ± 2.35	752.45 ± 83.25	73.91 ± 7.84	10.63 ± 1.02	19.87 ± 3.92	1670.17 ± 533.61	13.38 ± 1.99
	Cinnamomum camphora	0.5542 ± 0.17	5.47 ± 0.88	1209.72 ± 195.83	27.39 ± 1.60	45.45 ± 4.92	58.89 ± 4.20	500.56 ± 50.49	141.66 ± 20.44	3.84 ± 0.57	11.96 ± 1.69	9399.97 ± 6631.43	14.20 ± 3.46
	Manglietia fordiana	0.5536 ± 0.02	8.64 ± 1.89	1216.01 ± 212.04	25.58 ± 0.91	49.38 ± 9.51	63.26 ± 4.49	805.98 ± 166.78	67.91 ± 8.21	12.63 ± 3.74	14.95 ± 3.70	1257.35 ± 468.77	14.57 ± 2.00
	Nyssa sinensis	0.5460 ± 0.10	6.77 ± 1.24	1320.54 ± 398.51	25.07 ± 3.95	54.03 ± 8.30	60.98 ± 8.79	822.98 ± 254.27	85.94 ± 9.44	9.76 ± 2.15	23.70 ± 7.48	2685.52 ± 990.36	11.42 ± 4.58
	Mytilaria laosensis	0.5282 ± 0.03	11.37 ± 2.78	1581.30 ± 277.17	30.76 ± 6.25	54.44 ± 11.53	55.47 ± 3.43	1330.12 ± 278.26	75.94 ± 7.30	18.27 ± 3.51	25.67 ± 2.06	2362.18 ± 391.10	11.63 ± 1.29
	Michelia foveolata	0.5222 ± 0.03	7.67 ± 1.24	1189.92 ± 233.97	26.08 ± 2.82	46.43 ± 5.91	65.97 ± 2.93	732.02 ± 71.08	72.09 ± 6.88	10.53 ± 2.02	15.38 ± 3.39	1926.22 ± 860.69	14.96 ± 1.87
	Phoebe bournei	0.5138 ± 0.05	6.83 ± 1.85	1014.95 ± 142.4	20.95 ± 5.13	51.69 ± 9.05	74.16 ± 1.89	488.55 ± 65.30	95.59 ± 28.63	5.60 ± 1.33	9.40 ± 1.56	2679.74 ± 1721.04	14.04 ± 2.96
	Parakmeria lotungensis	0.4684 ± 0.08	7.48 ± 1.00	1333.98 ± 245.85	28.66 ± 4.85	47.62 ± 4.07	65.80 ± 3.61	667.01 ± 56.64	68.94 ± 8.68	10.19 ± 1.86	17.28 ± 4.03	1544.59 ± 410.55	14.15 ± 3.28
	Michelia chapensis	0.4392 ± 0.02	8.14 ± 1.13	1152.34 ± 225.2	27.00 ± 5.67	44.02 ± 3.56	57.35 ± 2.18	711.73 ± 85.44	82.33 ± 11.80	8.97 ± 0.95	27.43 ± 2.30	2988.26 ± 787.18	13.72 ± 1.45
	Michelia odora	0.4372 ± 0.06	8.14 ± 1.80	1209.94 ± 196.11	27.58 ± 3.54	45.91 ± 7.41	61.90 ± 4.37	724.24 ± 120.98	78.17 ± 16.26	9.92 ± 2.16	18.64 ± 4.27	1998.57 ± 641.67	13.34 ± 4.04
Coniferous trees	*Chamaecyparis pisifera*	0.4698 ± 0.09	7.23 ± 2.11	1643.78 ± 406.21	31.62 ± 3.23	53.68 ± 8.66	-	-	-	-	-	324.27 ± 206.63	20.71 ± 6.21
	Fokienia hodginsii	0.4321 ± 0.09	7.36 ± 2.25	1891.18 ± 691.94	35.51 ± 7.55	55.77 ± 13.48	-	-	-	-	-	478.12 ± 248.84	19.26 ± 7.53
	Taiwania cryptomerioides	0.3578 ± 0.11	8.99 ± 2.47	1944.15 ± 1206.24	44.58 ± 8.08	45.00 ± 22.00	-	-	-	-	-	306.39 ± 167.21	12.09 ± 3.46
	Cupressus lusitanica	0.3554 ± 0.03	13.61 ± 5.00	1519.01 ± 402.17	24.81 ± 4.40	64.35 ± 7.06	-	-	-	-	-	1954.48 ± 782.88	32.74 ± 6.11

Table 3. The wood microstructure cell characteristics of broad-leaf timber.

Trees	Type of Vessel Pore Combination	Type of Vessel Pore Arrangement	Wood Ray Type	Longitudinal Parenchyma Type	Wood Ray Spacing (μm)	The Number of Wood Rays
Dalbergia assamica	solitary pore or multiple pore	dispersing type	double row	solitary	80.07 ± 25.02	62.44
Altingia chinensis	solitary pore	dispersing type	uniseriate wood ray	solitary	88.06 ± 18.32	56.78
Castanopsis kawakamii	solitary pore or multiple pore	apsacline	uniseriate wood ray	solitary	50.65 ± 15.28	98.71
Michelia macclurei	multiple pore	dispersing type	multiseriate ray	solitary	160.64 ± 58.38	31.13
Michelia fallaxa	multiple pore	dispersing type	double row	solitary	117.99 ± 39.43	42.38
Cinnamomum camphora	pore cluster	dispersing type	double row	solitary	148.09 ± 37.05	33.76
Manglietia fordiana	multiple pore	dispersing type	double row	solitary	107.89 ± 44.05	46.34
Nyssa sinensis	multiple pore	dispersing type	double row	solitary	130.29 ± 21.20	38.38
Mytilaria laosensis	solitary pore or multiple pore	radial type	double row	solitary	129.91 ± 33.36	38.49
Michelia foveolata	multiple pore or pore cluster	dispersing type	double row	solitary	129.8 ± 51.16	38.52
Phoebe bournei	solitary pore	dispersing type	double row	solitary	171.56 ± 68.16	29.14
Parakmeria lotungensis	pore cluster or multiple pore	dispersing type	double row	solitary	125.82 ± 47.61	39.74
Michelia chapensis	pore cluster or multiple pore	radial type or dispersing type	double row	solitary	191.1 ± 57.97	26.16
Michelia odora	multiple pore or pore cluster	dispersing type	double row	solitary	119.33 ± 29.00	41.90
Chamaecyparis pisifera	-	-	-	-	132.28 ± 56.36	37.80
Fokienia hodginsii	-	-	-	-	157.5 ± 45.64	31.75
Taiwania cryptomerioides	-	-	-	-	154.11 ± 60.86	32.44
Cupressus lusitanica	-	-	-	-	235.49 ± 78.04	21.23

The wood ray cells in the coniferous trees were all uniseriate wood rays; that is, one cell wide. In broad-leaf trees, most ray cells are double rows that are two cells wide. *Altingia chinensis* and *Castanopsis kawakamii* exhibited a uniseriate type. *Michelia macclurei* has multiple rows of wood ray cells that are three cells wide. *Cinnamomum camphora* contains oil in its wood ray cells. The axial parenchyma of both coniferous and broad-leaf trees were scattered.

The width distance of the ray cells of the four coniferous trees ranged from 132.49 μm to 235.49 μm, while the number of ray cells within 5 mm was less compared to the 14 broad-leaved trees, ranging from 21.23 to 37.80. *Cupressus lusitanica* had the fewest wood rays (21.23). In broad-leaved trees, *Michelia chapensis* and *Phoebe bournei* had larger distances between wood rays, that is, 191.10 μm and 171.56 μm, respectively, and fewer numbers of wood rays, that is, 26.16 and 29.14, respectively, which is similar to coniferous trees. Meanwhile, *Altingia chinensis* and *Dalbergia assamica* had more than 50 rays, and *Castanopsis kawakamii* had the highest number of rays (98.71), meaning that these three types of broad-leaved species had a relatively high number of rays. Other broad-leaved species had fewer rays, ranging from 31.12 to 46.34.

3.3. Correlation between Wood Anatomical Properties of Broad-Leaf Trees

Analysis of the correlation between the characteristics of the 14 types of broad-leaf tree wood showed that there was a significant negative correlation between basic wood density and fiber width and vessel proportion (Table 4). Conversely, there was a significant positive correlation between basic wood density and vessel lumen area. These findings suggest that fiber width, vessel proportion, and vessel lumen area are the key factors influencing

basic wood density. Therefore, broad-leaf tree species with larger fiber widths and vessel proportions are likely to have lower basic wood densities. Meanwhile, species with larger vessel lumen areas may have higher basic wood densities.

Table 4. Correlation analysis of wood properties of broad-leaf trees.

Traits	Wood Basic Density	Fiber Length	Fiber Width	Fiber Length-Width Ratio	Fiber Proportion	Vessel Length	Vessel Width	Vessel Length-Width Ratio	Vessel Proportion	Vessel Lumen Area	Cell Wall
Fiber length	−0.01										
Fiber width	−0.27 **	0.54 **									
Fiber length-width ratio	0.18	0.72 **	−0.18								
Fiber proportion	0.15	−0.45 **	−0.34 **	−0.26 **							
Vessel length	−0.18	0.67 **	0.40 **	0.46 **	−0.48 **						
Vessel width	0.15	−0.01	0.10	−0.11	0.09	−0.26 **					
Vessel length-width ratio	−0.08	0.54 **	0.21 *	0.46 **	−0.37 **	0.88 **	−0.60 **				
Vessel proportion	−0.36 **	0.34 **	0.30 **	0.15	−0.78 **	0.52 **	−0.27 **	0.43 **			
Vessel lumen area	0.66 **	−0.16	−0.08	−0.10	0.10	−0.65 **	0.75 **	−0.66 **	−0.59 **		
Cell wall	0.04	0.74 **	0.22	0.71 **	−0.20	0.68 **	−0.54 **	0.76 **	0.18	−0.19	
Microfibril angle	0.01	−0.14	−0.04	−0.13	0.07	−0.19	−0.10	−0.06	−0.13	−0.16	−0.20

** $p < 0.01$, * $p < 0.05$.

There was a strong negative correlation between fiber content and fiber length, fiber width, vessel length, vessel length–width ratio, and vessel proportion. This suggests that tree species with higher fiber proportions tend to have thinner and shorter fibers and vessels as well as smaller vessel proportions. In contrast, fiber length was positively correlated with fiber width, vessel length, and vessel proportion. Therefore, tree species with longer fibers tended to have wider fibers, longer vessels, and higher vessel proportions. The length of the vessels had a strong negative correlation with the width of the vessels and the vessel lumen area. Conversely, a significant positive correlation was observed with the proportion of vessels. This suggests that tree species with longer vessels tend to have narrower vessels and a higher proportion of vessels.

3.4. Assessment of 14 Broad-Leaf Trees

Based on the results from the correlation analysis, wood species with higher basic density, longer fibers, narrower fibers, larger fiber tissue ratios, and smaller vessel tissue ratios were selected as the target criteria. Using a comprehensive index selection method, the wood properties of the 14 broad-leaved trees were evaluated, and the rankings of the comprehensive indices are listed in Table 5. Among them, *Dalbergia assamica* and *Castanopsis kawakamii* had a higher basic density, shorter and thinner fibers, higher fiber content, and lower vessel content. Therefore, the comprehensive index of these two tree species were ranked first and second, respectively. Although *Phoebe bournei* did not have an outstanding basic density, it had shorter and thinner fibers, the highest fiber content, and a relatively small vessel ratio, resulting in it being ranked third. *Altingia chinensis* had a relatively high basic density and the longest fibers, but it also had wider fibers and a higher vessel ratio. *Nyssa sinensis* had moderate basic density, fiber properties, and vessel properties. However, its microfibril angle was the smallest, ranking fifth. *Michelia macclurei*, *Michelia fallaxa*, *Manglietia fordiana*, *Michelia foveolata*, *Cinnamomum camphora*, *Mytilaria laosensis*, and *Parakmeria lotungensis* had similar wood properties. Their basic wood density, fibers, vessels, and microfibril angles were all moderate. In contrast, *Michelia odora* and *Michelia chapensis* had lower basic density, wider fibers, smaller fiber content, higher vessel content, and larger microfibril angles, resulting in their lower rankings in terms of the comprehensive index.

Table 5. Composite index of wood properties of different tree species.

No.	Tree Special	Wood Basic Density	Fiber Length	Fiber Width	Fiber Proportion	Vessel Proportion	Microfibril Angle	*I*
1	*Dalbergia assamica*	7.65	4.57	8.52	10.91	0.65	10.48	3.47
2	*Castanopsis kawakamii*	5.68	4.07	8.50	10.90	1.66	10.05	0.44
3	*Phoebe bournei*	4.48	4.77	7.96	11.12	1.41	12.08	−1.08
4	*Altingia chinensis*	5.93	7.60	10.19	8.60	3.14	10.78	−1.98
5	*Nyssa sinensis*	4.76	6.21	9.52	9.15	3.56	9.82	−2.79
6	*Michelia macclurei*	5.39	6.51	9.72	8.65	3.22	11.81	−4.20
7	*Michelia fallaxa*	5.29	6.29	9.80	8.41	2.98	11.51	−4.30
8	*Manglietia fordiana*	4.82	5.72	9.72	9.49	2.24	12.53	−4.47
9	*Michelia foveolata*	4.55	5.59	9.91	9.90	2.31	12.86	−5.04
10	*Cinnamomum camphora*	4.83	5.69	10.41	8.83	1.79	12.21	−5.07
11	*Mytilaria laosensis*	4.60	7.43	11.69	8.32	3.85	10.00	−5.19
12	*Parakmeria lotungensis*	4.08	6.27	10.89	9.87	2.59	12.17	−5.43
13	*Michelia odora*	3.81	5.69	10.48	9.28	2.80	11.47	−5.97
14	*Michelia chapensis*	3.83	5.42	10.26	8.60	4.11	11.80	−8.33

4. Discussion

Global demand for precious hardwoods has significantly increased, leading to a severe shortage of valuable broad-leaved tree resources. The supply–demand contradiction has become increasingly prominent. The subtropical region of China harbors several promising tree species. With abundant water and thermal resources, favorable edaphic conditions exist for the growth and development of valuable tree species. However, these resources need to be fully explored.

The basic density of wood is a comprehensive indicator influenced by various wood properties and has a direct relationship with the hardness and strength of wood. Therefore, the basic density of wood is important for its processing and use [14]. Precious tree species have excellent material quality mainly because of their high wood density, beautiful color, and texture. In the present study, the basic wood density of the 29-year-old *Dalbergia assamica* was the highest, reaching >0.85 g·cm^{-3}. This result was consistent with the wood basic density of *Dalbergia* species and higher than the wood basic density of 15-year-old *Dalbergia odorifera* (0.715 g·cm^{-3}) [15]. Therefore, if the plantation site for *Dalbergia assamica* is chosen appropriately, it has strong prospects for development. The wood basic density of 39-year-old *Altingia chinensis* was 0.6812 g·cm^{-3}, which was consistent with the wood basic density of 92-year-old *Altingia gracilipes* (0.62 g·cm^{-3}) [16]. *Altingia chinensis* plantations grow faster [17], and artificial cultivation technology is mature. It is a broad-leaved tree species suitable for the cultivation of large-diameter timber. In this study, the wood basic density of 35-year-old *Castanopsis kawakamii* was 0.652 g·cm^{-3}, similar to that of *Altingia chinensis*. *Castanopsis kawakamii* has straight trunks and grows rapidly with a maximum annual growth rate of 1 cm. The wood basic density of 40-year-old *Castanopsis kawakamii* has been found to be 0.584 g·cm^{-3} [18], which was higher than the result of this study, mainly due to site conditions. Therefore, further research is needed to determine the optimal seed source area for *Castanopsis kawakamii* wood. The wood basic density of *Michelia odora* and *Michelia chapensis* was below 0.5 g·cm^{-3}, similar to that of 24-year-old *Pinus massoniana* wood (0.43 g·cm^{-3}). *Michelia odora* is an endangered plant and expanding artificial breeding scales should be prioritized to address resource endangerment issues. Although the basic density of *Michelia chapensis* wood was relatively low, it had a rapid growth rate with an average annual diameter growth of 0.9 cm [19]. However, their properties are unclear, and genetic improvements in wood properties have not yet begun, thus requiring further research. *Parakmeria lotungensis* is a precious timber species that has been discovered in recent years with a slow growth rate [3]. In this study, the basic wood density of 36-year-old

Parakmeria lotungensis was 0.49 g·cm^{-3}. However, the wood basic density of 26-year-old *Parakmeria lotungensis* was found to be 0.63 g·cm^{-3}, which is higher than the result of this study [3]. Therefore, further research is needed to understand the relationship between the wood properties of *Parakmeria lotungensis* and age.

The fiber length and fiber length–width ratio significantly affected the bending and tensile strength of the wood. For instance, in the context of pulp materials, wood with a higher fiber aspect ratio tends to enhance the glossiness and smoothness of paper [20]. According to the grading standards defined by the International Association of Wood Anatomists [14], among the 14 tested broad-leaf trees, only the fibers of *Altingia chinensis* were classified as moderately long fibers (1616.24 μm). This has surpassed the fiber length of 12-year-old poplar trees (830~1270 μm) [21] and 23-year-old *Eucalyptus grandis* (986~1110 μm) [22]. The fiber lengths of the remaining 13 broad-leaf trees fell within the range of medium length (900~1600 μm). The proportion of fiber in all 14 broad-leaf trees was above 50%, which is similar to that of 23-year-old *Eucalyptus grandis* (51.80%~58.70%) [22]. This indicated that these broad-leaf trees were suitable for fiber applications.

The diameter, proportion, and arrangement of vessels collectively affect the strength and hardness of wood, whereas the vessel type influences the texture of the wood [23]. Currently, there are no specific vessel-grading standards. Typically, vessels with lengths less than 350 μm are considered short, those between 350 μm and 800 μm are categorized as medium, and those exceeding 800 μm are classified as long [23]. The results of this study have shown that *Dalbergia assamica* had the shortest vessels, shorter than the vessel lengths of 23-year-old *Eucalyptus grandis* (429.18~480.43 μm) [22]. Meanwhile, *Mytilaria laosensis* possessed the longest vessels, surpassing the vessel length of 54-year-old *Schima superba* (1297.34 μm) [7]. The transportation of water through vessels is the primary factor influencing the growth of tropical tree species [24]. The vessel proportions of *Michelia chapensis*, *Mytilaria laosensis*, *Nyssa sinensis*, *Michelia macclurei*, and *Altingia chinensis* were relatively high, accounting for more than 20% of their composition. These proportions are similar to those of popular methods, which range from 21.40% to 29.99% [25]. The vessel proportions of *Michelia fallaxa* (19.87%), *Michelia odora* (18.64%), *Parakmeria lotungensis* (17.28%), *Michelia foveolate* (15.38%), and *Manglietia fordiana* (14.95%) were similar to those of *Eucalyptus grandis*, ranging from 15.40% to 17.2% [22]. In contrast, tree species such as *Cinnamomum camphora*, *Phoebe bournei*, and *Dalbergia assamica* had relatively low vessel contents. This is because tree species with low vessel proportions generally adapt to the humid climate of subtropical regions and fulfill their growth requirements by having larger vessel diameters [26].

The microfibril angle was negatively correlated with wood strength. Smaller microfibril angles are associated with a greater tensile strength [27]. In the present study, there was little variation in the microfibril angles among the 14 broad-leaved tree species, ranging from 11.42° to 14.96°, indicating a certain level of tensile strength. The microfibril angle of *Nyssa sinensis* (11.42°), *Mytilaria laosensis* (11.63°), and *Castanopsis kawakamii* (11.68°) was higher than that of 6-year-old *Phyllostachys pubescens* (8.17°~10.51°) [28], lower than that of 2-year-old *Populus deltoides* (averaging 14.1°) [29], and lower than that of 10-year-old poplar (ranging from 16.34° to 19.16°) [26]. A similar microfibril angle has been observed in 7-year-old *Cyclocarya paliurus* (11.0°~15.2°) [30]. *Nyssa sinensis* (11.42°), *Mytilaria laosensis* (11.63°), and *Castanopsis kawakamii* (11.68°) exhibited relatively high tensile strengths. However, further research is needed to investigate the relationship between the microfibril angle and age, provenance, and genetics. Among the four coniferous tree species, *Taiwania cryptomerioides* had a smaller microfibril angle, similar to that of broad-leaved trees, distinguishing it from the other three coniferous species. *Taiwania cryptomerioides* has straight trunks, rapid growth, and a beautiful wood color and texture. The bending strength and surface hardness of *Taiwania cryptomerioides* wood are higher than those of *Cunninghamia lanceolata*, and its growth rate is faster than that of *Cunninghamia lanceolata* [31]. However, to date, there have been relatively few studies on the properties of *Taiwania cryptomerioides* wood, and more samples should be used to verify these findings.

Wood rays are composed of thin-walled cells that form the weaker parts, especially in broad-leaf trees with well-developed wood rays. Wood is prone to cracking along the direction of its rays, which affects its usability [32]. In the field of wood science, the average number of wood rays within a 5 mm range is commonly used to evaluate the extent of cracking caused by wood rays. Wood rays numbering 25 or fewer are considered a relatively low number, whereas those ranging from 25 to 50 are considered a low number [23,33]. This study has shown that the number of wood rays in 14 species of broad-leaf trees was higher compared to four conifer tree species. The wood rays of these 14 broad-leaf tree species were mostly double rows with a width of 2–3 cells. *Altingia chinensis*, *Dalbergia assamica*, and *Castanopsis kawakamii*, which have higher wood densities, also exhibited a higher count of wood rays, indicating increased susceptibility to cracking. In contrast, *Michelia chapensis* and *Phoebe bournei* have lower densities but fewer wood rays, making them less prone to cracking. The wood from *Chamaecyparis pisifera*, *Fokienia hodginsii*, *Taiwania cryptomerioides*, and *Cupressus lusitanica* was lightweight and soft. Compared with broad-leaf wood, it is less susceptible to cracking. Significant differences have been found in wood rays between the juvenile and mature wood of *Pinus massoniana* and *Cunninghamia lanceolata* [33]. Therefore, to more effectively understand wood processing, it is necessary to further investigate the differences between the mature and juvenile woods of these species.

The performance of wood is influenced by the nature of its properties. Understanding the correlations between these properties helps evaluate the overall quality and suitability of wood [20]. The basic density of wood is a relatively easy-to-obtain parameter that serves as an indicator of overall wood performance. This study found that the fiber width, vessel proportion, and vessel lumen diameter may be the primary factors influencing basic wood density. These findings provide a scientific basis for the processing and use of wood. Fiber width and conduit diameter can potentially weaken the wood structure's support capacity [26]. Vessel lumen diameter can be attributed to the growth environment of different tree species, particularly their adaptation to rainfall, moisture, and genetics [34].

A comprehensive index selection is an evaluation approach that combines multiple traits. This evaluation method is comprehensive and has high selection efficiency [35]. Construction, furniture, and fiberboard materials require wood with high density, abundant fiber content, and small microfiber angles, which are considered excellent materials [25,36]. In this study, a comprehensive index selection method was used for evaluation. *Dalbergia assamica*, which grows in high-altitude areas, is a heavyweight timber with dense wood. However, they contain numerous wooden rays and are prone to cracking. *Castanopsis kawakamii*, *Phoebe bournei*, and *Altingia chinensis*, on the other hand, have high hardness and fiber content among broad-leaf woods, making them suitable for furniture and construction materials. Eight broad-leaf trees, including *Nyssa sinensis*, *Michelia macclurei*, *Michelia fallaxa*, *Manglietia fordiana*, *Michelia foveolata*, *Cinnamomum camphora*, *Mytilaria laosensis*, and *Parakmeria lotungensis*, had moderate growth rates and were classified as medium wood with easy workability. *Michelia odora* and *Michelia chapensis* have well-developed vessels and a high percentage of vessel elements, similar to conifers in terms of wood hardness and ease of processing. However, they are not suitable as valuable broadleaf materials. The quality of wood is determined by multiple indicators. However, the superiority or inferiority of a single indicator cannot determine its quality. Therefore, further exploration should be conducted on the physical properties of wood, such as bending strength and tensile strength, chemical properties such as lignin content, cellulose content, and extractives, and other indicators, to fully evaluate broad-leaf woods.

5. Conclusions

The findings have indicated significant variations in wood anatomical properties and microstructures among the 14 broad-leaf trees, offering valuable support for the diverse applications of broad-leaf timber. The main factors influencing basic wood density were the fiber width, vessel proportion, and vessel lumen area. *Parakmeria lotungensis* and *Michelia chapensis* were found to have a wood basic density below 0.45 g·cm^{-3}, rendering them

unsuitable as valuable tree species. In contrast, *Dalbergia assamica*, *Altingia chinensis*, and the remaining 11 broad-leaf species were excellent sources of fiber materials.

Author Contributions: Y.W. (Yunpeng Wang): data curation, methodology, software, formal analysis, and writing—original draft. Y.W. (Yiping Wang): investigation and resources. L.S.: writing—review and editing. Z.W., H.L., M.H., Q.L. and C.C.: investigation. X.H.: resources and investigation. X.H.: resources, investigation, funding acquisition, conceptualization, and project administration. Y.Z.: investigation, methodology, conceptualization, data curation, writing—review and editing, supervision, project administration, and funding acquisition. All authors have read and agreed to the published version of the manuscript.

Funding: This research was funded by the Key Industrial Technology Research Project of Jiangxi Academy of Sciences (2021YSBG10002), the Key Research and Development Plan Project of Provincial-Level Scientific Research Project Funding Overall Contract System Pilot Demonstration Project of Jiangxi Academy of Sciences (2022YSBG21003), the Scientific Research Funding of Provincial Talent Training of Jiangxi Academy of Sciences (2023YRCS004), and National Government Guidance Fund for Regional Science and Technology Development (20192ZDD01004).

Data Availability Statement: The data are available upon request from the corresponding author.

Conflicts of Interest: The authors declare no conflict of interest.

References

1. Zhang, Q.; Qi, J.C.; Cheng, B.D.; Yu, C.; Liang, S.; Wiedmann, T.O.; Liu, Y.; Zhong, Q.M. Planetary boundaries for forests and their national exceedance. *Environ. Sci. Technol.* **2021**, *55*, 15423–15434. [CrossRef] [PubMed]
2. Zhang, S.B.; Slik, J.W.F.; Zhang, J.L.; Cao, K.F. Spatial patterns of wood traits in China are controlled by phylogeny and the environment. *Glob. Ecol. Biogeogr.* **2011**, *20*, 241–250. [CrossRef]
3. Chappin, M.M.H.; Cambre, B.; Vermeulen, P.A.M.; Lozano, R. Internalizing sustainable practices: A configurational approach on sustainable forest management of the Dutch wood trade and timber industry. *J. Clean. Prod.* **2015**, *107*, 760–774. [CrossRef]
4. Zhang, Q.; Li, Y.; Yu, C.; Qi, J.; Yang, C.; Cheng, B.; Liang, S. Global timber harvest footprints of nations and virtual timber trade flows. *J. Clean. Prod.* **2020**, *250*, 119503.1–119503.11. [CrossRef]
5. Xiang, W.; Liu, S.; Lei, X.; Frank, S.C.; Tian, D.; Wang, G.; Deng, X.W. Secondary forest floristic composition, structure, and spatial pattern in subtropical China. *J. For. Res.* **2013**, *18*, 111–120. [CrossRef]
6. Jiang, Z. Current situation and future development: The forest products industry in China. *For. Prod. J.* **2007**, *57*, 7–8.
7. Wang, Y.P.; Zhang, R.; Zhou, Z.Z. Radial variation of wood anatomical properties determines the demarcation of juvenile-mature wood in *Schima superba*. *Forests* **2021**, *12*, 512. [CrossRef]
8. Cardoso, S.; Sousa, V.B.; Quilhó, T.; Pereira, H. Anatomical variation of teakwood from unmanaged mature plantations in East Timor. *J. Wood Sci.* **2015**, *61*, 326–333. [CrossRef]
9. Wang, H.H.; Drummond, J.G.; Reath, S.M.; Hunt, K.; Watson, P.A. An improved fibril angle measurement method for wood fibres. *Wood Sci. Technol.* **2001**, *34*, 493–503. [CrossRef]
10. Bonham, V.A.; Barnett, J.R. Fibre length and microfibril angle in silver birch (*Betula pendula* roth). *Holzforschung* **2001**, *55*, 159–162. [CrossRef]
11. Abdullah, N.; Tabet, T.A.; Aziz, F. Regression models on the age-affecting and microfibril angle of *Acacia mangium*. *J. Indian Acad. Wood Sci.* **2010**, *7*, 49–53. [CrossRef]
12. Cheng, J.Q. *Wood Science*; China Forestry Publishing House: Beijing, China, 1985; pp. 55–56.
13. Cotterill, P.P.; Dean, C.A. *Successful Tree Breeding with Index Selection*; CSIRO, Division of Forestry and Forest Products: Victoria, Australia, 1990; pp. 53–56.
14. Committee, I.H. IAWA list of microscopic features for hardwood identification. *IAWA J.* **2004**, *10*, 176–219.
15. Yu, M.; Liu, K.; Zhou, L.; Zhao, L. Testing three proposed DNA barcodes for the wood identification of *Dalbergia odorifera* T. Chen and *Dalbergia tonkinensis* Prain. *Holzforschung* **2016**, *70*, 127–136. [CrossRef]
16. Zhang, D.B.; Zhou, C.M.; Wu, X.L. Study on wood physical and mechanical properties of *Altingia gracilipessl*. *Hunan For. Sci. Technol.* **2018**, *5*, 86–89.
17. Ye, X.; Zhang, M.; Jiang, Y.; Fan, H.; Liu, B. The complete chloroplast genome of *Altingia chinensis* (Hamamelidaceae). *Mitochondrial DNA B* **2020**, *5*, 1808–1809. [CrossRef]
18. Buajan, S.; Liu, J.F.; He, Z.S.; Feng, X.P.; Muhammad, A. Effects of gap size and locations on the regeneration of *Castanopsis kawakamii* in a subtropical natural forest, China. *J. Trop. For. Sci.* **2018**, *30*, 39–48.
19. Wang, R.; Hu, D.; Zheng, H.; Yan, S.; Wei, R.P. Genotype × environmental interaction by AMMI and GGE biplot analysis for the provenances of *Michelia chapensis* in South China. *J. For. Res.* **2016**, *27*, 659–664. [CrossRef]
20. Liu, Y.; Zhou, L.; Zhu, Y.; Liu, S. Anatomical features and its radial variations among different *Catalpa bungei* clones. *Forests* **2020**, *11*, 824. [CrossRef]

21. Fang, S.Z.; Yang, W.Z.; Fu, X.X. Variation of microfibril angle and its correlation to wood properties in poplars. *J. For. Res.* **2004**, *15*, 261–267.
22. Palermo, G.P.D.M.; Latorraca, J.V.D.F.; De Carvalho, A.M.; Calonego, F.W.; Severo, E.T.D. Anatomical properties of *Eucalyptus grandis* wood and transition age between the juvenile and mature woods. *Eur. J. Wood Wood Prod.* **2015**, *73*, 775–780. [CrossRef]
23. Xu, Y.M. *Wood Science*; China Forestry Publishing House: Beijing, China, 2006; pp. 60–61.
24. Poorter, L.; Mcdonald, I.; Alfredo, A.; Fichtler, E.; Juan-Carlos, L.; Marielos, P.-C.; Sterck, F.; Villegas, Z.; Sass-Klaassen, U. The importance of wood traits and hydraulic conductance for the performance and life history strategies of 42 rainforest tree species. *New Phytol.* **2010**, *185*, 481–492. [CrossRef] [PubMed]
25. Fang, S.Z.; Yang, W.Z. Interclonal and within-tree variation in wood properties of poplar clones. *J. For. Res.* **2003**, *14*, 263–268.
26. Pacheco, A.; Camarero, J.J.; Carrer, M. Linking wood anatomy and xylogenesis allows pinpointing of climate and drought influences on growth of coexisting conifers in continental Mediterranean climate. *Tree Physiol.* **2015**, *36*, 502–512. [CrossRef] [PubMed]
27. Jäger, A.; Bader, T.; Hofstetter, K.; Eberhardsteiner, J. The relation between indentation modulus, microfibril angle, and elastic properties of wood cell walls. *Compos. Part A Appl. Sci. Manuf.* **2011**, *42*, 677–685. [CrossRef]
28. Wang, X.Q.; Li, X.Z.; Ren, H.Q. Variation of microfibril angle and density in moso bamboo (*Phyllostachys pubescens*). *J. Trop. For. Sci.* **2010**, *22*, 88–96.
29. Wang, Y.R.; Liu, C.W.; Zhao, R.J.; McCord, J.; Rials, T.; Wang, S.Q. Anatomical characteristics, microfibril angle and micromechanical properties of cottonwood (*Populus deltoides*) and its hybrids. *Biomass Bioenerg.* **2016**, *93*, 72–77. [CrossRef]
30. Deng, B.; Fang, S.Z.; Yang, W.X.; Tian, Y.; Shang, X.L. Provenance variation in growth and wood properties of juvenile *Cyclocarya paliurus*. *New Forest.* **2014**, *45*, 625–639. [CrossRef]
31. Wang, Q.H.; Li, Y.Q.; Yuan, X.L.; Wang, Y. The complete chloroplast genome sequence of *Taiwania flousiana*. *Mitochondrial DNA B* **2020**, *5*, 1040–1041. [CrossRef]
32. Ma, L.Y.; Meng, Q.L.; Jiang, X.M.; Ge, Z.D.; Cao, Z.X.; Wei, Y.P.; Guo, J. Spatial organization and connectivity of wood rays in *Pinus massoniana* xylem based on high-resolution μCT-assisted network analysis. *Planta* **2023**, *258*, 28. [CrossRef]
33. Meng, Q.; Fu, F.; Wang, J.; He, T.; Jiang, X.; Zhang, Y.; Yin, Y.; Li, N.; Guo, J. Ray traits of juvenile wood and mature wood: *Pinus massonia* and *Cunninghamia lanceolata*. *Forests* **2021**, *12*, 1277. [CrossRef]
34. Nocetti, M.; Rozenberg, P.; Chaix, G.; Macchioni, N. Provenance effect on the ring structure of teak (*Tectona grandis* L.f.) wood by X-ray microdensitometry. *Ann. For. Sci.* **2011**, *68*, 1375–1383. [CrossRef]
35. White, T.L.; Adams, W.T.; Neale, D.B. *Forest Genetics*; Science Press: Beijing, China, 2013; pp. 115–119.
36. Yang, Z.; Xia, H.; Tan, J.; Feng, Y.H.; Huang, Y.L. Selection of superior families of *Pinus massoniana* in southern China for large-diameter construction timber. *J. For. Res.* **2020**, *31*, 475–484. [CrossRef]